SAND2022-2598C

Draft SPIE proceeding for Defense and Commercial Sensing conference, Orlando, April 2022

Radiation damage and mitigation by minority carrier injection in GaSb/InAs and InAsSb/AlAsSb heterojunction barrier infrared detectors

C. J. Fredricksen,[1] R. E. Peale,[1,2] N. Dhakal,[2] C. L. Barrett,[1] T. O. Boykin II,[1] D. Maukonen,[1] L. Davis,[2] B. Ferarri,[2] L. Chernyak,[2] O. A. Zeidan,[3] S. D. Hawkins,[4] J. F. Klem,[4] Sanjay Krishna,[5] Alireza Kazemi,[5] Ted Schuler-Sandy[6]

1) Truventic LLC, Orlando FL
2) University of Central Florida, Orlando FL
3) Orlando Health, Orlando FL
4) Sandia National Laboratories, Albuquerque NM
5) Ohio State University, Columbus OH
6) University of New Mexico, Albuquerque NM

Abstract

Effects of gamma and proton irradiation, and of forward bias minority carrier injection, on minority carrier diffusion and photoresponse were investigated for long-wave (LW) and mid-wave (MW) infrared detectors with engineered majority-carrier barriers. The LWIR detector was a type-II GaSb/InAs strained-layer superlattice pBiBn structure. The MWIR detector was a InAsSb/AlAsSb nBp structure without superlattices. Room temperature gamma irradiations degraded the minority carrier diffusion length of the LWIR structure, and minority carrier injections caused dramatic improvements, though there was little effect from either treatment on photoresponse. For the MWIR detector, effects of room temperature gamma irradiation and injection on minority carrier diffusion and photoresponse were negligible. Subsequently, both types of detectors were subjected to gamma irradiation at 77 K. In-situ photoresponse was unchanged for the LWIR detectors, while that for the MWIR ones decreased 19% after cumulative dose of ~500 krad(Si). Minority carrier injection had no effect on photoresponse for either. The LWIR detector was then subjected to 4 Mrad(Si) of 30 MeV proton irradiation at 77 K, and showed a 35% decrease in photoresponse, but again no effect from forward bias injection. These results suggest that photoresponse of the LWIR detectors is not limited by minority carrier diffusion.

2.0 INTRODUCTION

Radiation hardened infrared detectors are needed for interceptor seekers [1]. In this application, detectors accumulate radiation damage from environmental sources [2] or potential single events. Radiation damage degrades infrared detector performance, which we seek to reverse via in-situ, remotely-applied mitigation treatments.

Forward bias minority-carrier injection has been shown to provide long-lasting recovery to the photoresponse of radiation-damaged wide-gap p-i-n UV photodiodes [3,4]. In such devices, UV absorption occurs in the top-most layer, which is purposely thinned to improve collection of photo-generated minority carriers since these must diffuse to the junction. Hence, minority carrier diffusion length (L) affects quantum efficiency of these simple devices. Radiation damage reduces minority carrier lifetime and hence diffusion length and quantum efficiency. Forward bias injection passivates the radiation-defect recombination centers that lower lifetime. The benefit to photoresponse can last hours to days, and this effect is correlated with direct measurements of diffusion length by the electron-beam induced current (EBIC) technique.

We hypothesized that similar radiation defect mitigation by forward bias minority carrier injection might occur in modern MW- and LW-IR heterojunction barrier detectors formed by epitaxial growth of layered semiconductors. Initial experiments [5,6] on unprocessed MWIR pBn, pBiBn, and pBp Type II GaSb/InSb strained-layer-superlattice detector wafers, with bottom contact made to the substrate backside, showed promising results. Namely, EBIC scans across the cleaved edges of wafers showed an exponential decay from an EBIC peak near the contact/absorber interface as the electron beam scanned into the substrate, where the characteristic decay length is interpreted to give the value of L. After room temperature gamma irradiation, the diffusion length decreased significantly, but forward bias injection increased it by up to several times [5,6]. Corresponding improvements were seen in the unbiased room-temperature photoresponse of the unprocessed wafers at 4 μm wavelength. The benefits lasted hours to days [5,6]. These preliminary samples differ from processed detectors in top and bottom contact fabrication method. Furthermore, actual detectors are operated at cryogenic temperatures and under reverse bias, and the environmental radiation damage they suffer occurs under these operational conditions.

This paper reports results of experiments on type II GaSb/InAs strained-layer superlattice LWIR pBiBn and InAsSb/AlAsSb MWIR nBp structures and processed detectors. The MWIR structure comprised simple layers without superlattices. EBIC was performed across the edge of cleaved unprocessed wafers comprising epi-layers on substrate, as before. However, all photoresponse measurements were done on processed detectors in a liquid-nitrogen optical cryostat. For the LWIR detectors, initial room temperature irradiations did degrade the diffusion length, and it improved after forward bias injection, but effects of either treatment on photoresponse were insignificant. For the MWIR detectors, room-temperature irradiation and injection had negligible effect on both minority carrier diffusion and photoresponse.

Much of the radiation damage might be expected to anneal out at room temperature. To avoid this, a set of gamma and proton irradiations were performed with detectors maintained at liquid-nitrogen temperature. Photoresponse and injection effects were studied after intermediate doses without warming up. The MWIR detector response degraded 19% after cumulative gamma dose of nearly 500 krad(Si). The LWIR detector response was unchanged up to over 700 krad(Si). Neither detector's photoresponse showed any effect following in-situ forward bias injection.

Next, the LWIR detectors were subjected to proton irradiation at 77 K, which caused a 35% decrease in photoresponse after 4 Mrad(Si) dose. Again, there was no change to photoresponse caused by forward bias injection.

These results for the LWIR detectors suggest that their photoresponse is not limited by minority carrier diffusion. For the MWIR detectors, the decrease in response after gamma irradiation can be attributed to degraded minority carrier diffusion only if such occurs at 77 K that was absent at room temperature.

Experimental details

The LWIR structure studied was pBiBn GaSb/InAs type II strained layer superlattice fabricated at Ohio State University (OSU) and designated G13-141. The epi-layers grown on GaSb substrate comprise a p^+ bottom contact, a barrier layer, a low-doped p-type absorber of 1.9 μm thickness, another barrier layer, and an n^+ top contact. Each of these regions comprise a superlattice formed from layers of InAs, GaSb, and InSb materials. The precise details have not been approved for public disclosure. The sequence of room temperature irradiations on G13-141

comprised 1.1 krad(Si) of 80 MeV protons (Orlando Health Cyclotron), followed by 55, 108, and 414.5 krad(Si) doses of ^{60}Co gamma irradiation (Steris). EBIC, blackbody photoresponse, and spectral photoresponse were all measured at 77 K before and after each irradiation. We observed no significant increase in photoresponse or noise under reverse bias, so all measurements were performed without bias.

The MWIR structure studied was a nBp InAsSb/AlAsSb structure fabricated by Sandia National Laboratories on GaSb substrate and designated EB3108 [7]. The n-type InAsSb absorber is 2 μm thick. Between the absorber and the p^+ InAsSb top contact is an AlAsSb barrier to majority-carriers (electrons). In contrast to the LWIR detector, none of the regions comprise a superlattice. The maximum photoresponse is achieved already at zero-bias, when the InAsSb depletion width is ~0.15 μm [7], so measurements were performed unbiased. The sequence of room temperature irradiations included 55 krad(Si) gamma on EBIC samples only, then 108 and 414.5 krad(Si) gamma on both EBIC and detector samples. These irradiations were followed by EBIC, broadband photoresponse, and spectral photoresponse measurements.

The EBIC measurements used a scanning electron microscope (SEM) with temperature-controlled stage. Only 77 K EBIC data are discussed here. EBIC samples were unprocessed epi-layers on substrate, which were cleaved to dimensions of ~1 cm^2. Both sides were blanket coated with gold on a Ti sticking layer then cleaved again, with EBIC performed across this cleaved edge. The electron beam is scanned from the top contact inward through the epi-layers and into the substrate, and a peak is observed. The peak is assumed to occur at the junction between absorber and top-contact layer. No EBIC signal is observed when scanning near the bottom contact. Forward-bias injection is applied using a parameter analyzer.

Photoresponse was measured on processed detectors using a chopped blackbody source (200 or 300 ^{o}C). The blackbody spectrum at these temperatures peaks at 6.5 or 5.2 μm wavelength, respectively, which are below the G13-141 cutoff, and beyond for EB3108. The detector dies included multiple detectors of different size and shape. The G13-141 detectors were free mesas with passivated sidewalls, and the EB3108 detectors used unpassivated etched mesas. Detector dies were mounted with indium to ceramic leadless chip carriers (LCC). Individual detectors were wire bonded to the LCC contacts. The LCC was snapped into a socket surface-mounted on a printed circuit board, which had been milled out to allow an aluminum cold finger to thermally contact the LCC via Apiezon-N grease. The cold finger was mounted to the cold plate of a liquid nitrogen cryostat with ZnSe window. Chopped signals from the detectors were cabled via hermetic multipin connectors to a Stanford Research SR570 current preamplifier with built-in bias capability and band-pass filtering. The output was synchronously amplified by an SR530 lock-in, whose output was recorded via Labview. A total of nine detectors were monitored on each die. All the detectors of a given type behaved similarly, and the magnitude of their response was proportional to detector area.

For infrared experiments, the operating bias (usually zero) could be switched to a forward bias minority-carrier-injection treatment using a Keithley source meter. Experiments were facilitated by switching between measurement and treatment via a Labview-controlled relay box. Forward bias injected charge was increased in steps from 0.01 to 200 mA-s/mm^2, with each injection followed by photoresponse measurement. Untreated control detectors on the same die were simultaneously monitored.

For spectral photoresponse, the preamplified, interferometer-modulated signal was fed to a custom interface box for a Bomem DA8 Fourier spectrometer with globar source and KBr

beamsplitter. The detector cryostat optical-access tailstock was o-ring muff-coupled into the vacuum sample compartment. The spectra were uncorrected for the spectral function of source and beamsplitter.

Following the room temperature irradiation studies, a set of low-temperature irradiation and in-situ responsitivity measurements and injection treatments was performed using a liquid nitrogen cryostat. A platinum resistor (PT-100) embedded in the cryostat cold finger monitored temperature. Gamma irradiation, facilitated by 5th Gait Technologies, was performed at Radiation Test Solutions (Colorado Springs) using their High Dose Rate source. Timed irradiations were performed with the cryostat window touching the housing of the retractable ^{60}Co source, where the dose rate was 50 rad(Si)/s. After the source retraction, the cryostat could be immediately removed to a photoresponse/treatment test set up comprising blackbody source, chopper, preamp, lock-in amplifier, source meter, relay box, and labview computer. Photoresponse was measured before and after each exposure. Forward bias injection experiments began only after the later doses.

Low temperature proton irradiations were performed on G13-141 detectors at the Texas A&M University (TAMU) K150 cyclotron. The proton beam passed through the ZnSe cryostat window before impinging on the detectors. The 30 MeV energy at the sample and the dose after each timed irradiation were determined by facility staff. An accumulated dose of 3.966 Mrad(Si) was applied over the course of about 12 hours while the detectors were maintained at 77 K throughout. A remotely-controlled off-axis parabolic flip mirror allowed the sample to view the 300 °C blackbody for photoresponse measurements after each timed irradiation without moving the cryostat, giving highly repeatable optical alignment.

RESULTS AND DISCUSSION

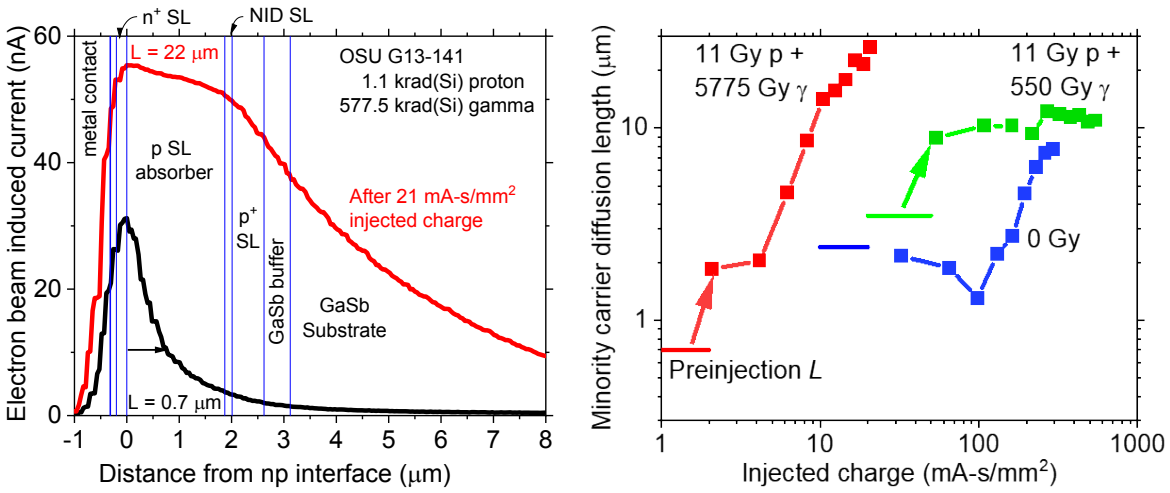

Figure 1. (1eft) EBIC curves for OSU G13-141 after irradiation. (right) Minority carrier diffusion length within the absorber layer vs injected charge density.

Figure 1 (left) presents 77 K EBIC scans on unbiased G13-141 after 1.1 krad(Si) proton and cumulative 577.5 krad(Si) gamma room-temperature irradiation doses. The characteristic diffusion length L = 0.7 μm (assuming exponential decay) for the as-irradiated sample is less than

half of the thickness of the absorber. This suggests that any depletion width and built-in field extends even less into the absorber, and that the EBIC is limited by minority carrier diffusion. This contrasts with other p-i-n structures we have studied, where the EBIC signal is flat across the entire absorber, falling rapidly to zero as the beam enters the substrate. After a forward bias injection of 21 mA-s/mm^2, L increased to 22 μm. The collected current for minority carriers excited near the top of the absorber increases two-fold. For carriers excited at the bottom of the absorber the improvement is 14-fold. Within the substrate, the decay length remains at about 4 μm, unchanged by injection.

Figure 1 (right) presents a plot of L vs injected charge for samples before and after a total 80 MeV 1.1 krad(Si) proton dose plus cumulative gamma doses of 55.0 or 577.5 krad(Si) for G13-141. Irradiation decreases L, while treatment recovers it. The points at zero injected charge show that the maximum irradiation degraded L by a factor of almost 4x. The difference between un-irradiated and low-dosed values is within the uncertainty determined by the scatter. The most heavily irradiated sample's L improves with injected charge much more than for the unirradiated or low-dosed samples. The achieved improvement for the irradiated sample is 31x, while that of the virgin and low-dosed samples is only ~3x. In each case, injection treatment caused L to become much greater than the absorber layer thickness.

For EB3108, the minority carrier diffusion length determined by EBIC is ~1 μm, which is much greater than the zero-bias depletion width and about half the absorber thickness. Hence, EBIC is also diffusion limited for EB3108. In contrast to G13-141, the EBIC curves are unaffected by irradiation or injected charge up to the highest room temperature gamma dose received, within the 20% uncertainty determined by the scatter. The difference in susceptibility to radiation for the two structures may be due to differences in absorber design, e.g. the presence or absence of superlattices or the different materials used.

Figure 2 (left) presents a plot of diffusion length as a function of time following forward-bias injection for G13-141 after room temperature proton and 55.0 krad(Si) of gamma irradiation. The horizontal line indicates the pre-treatment diffusion length value near 3.5 μm, and forward bias injection has increased the minority carrier diffusion length to 11 μm (see Fig. 1, right). The sample is maintained at 77 K in the SEM, and an EBIC scan is measured after several time intervals until the diffusion length has relaxed to its pretreatment level. The benefits to diffusion length of forward-bias injection treatment last four hours at 77 K.

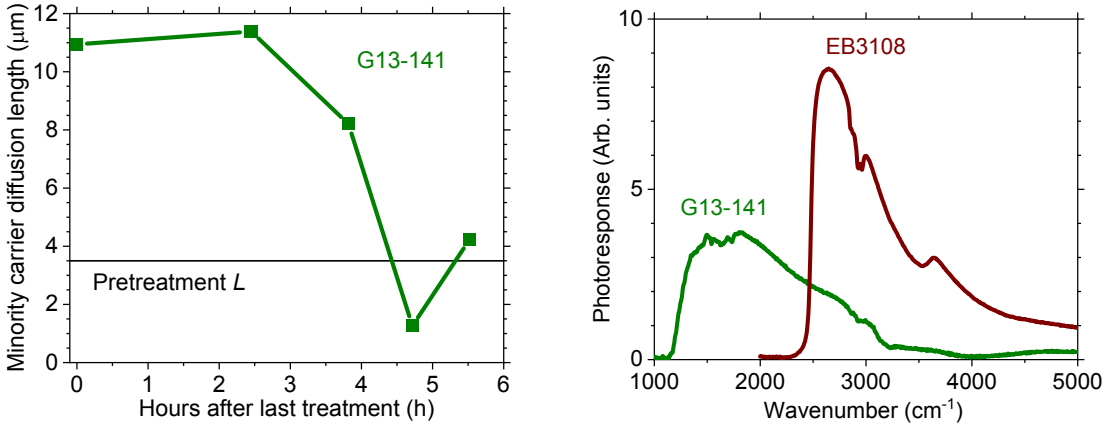

Figure 2. (left) Mitigation treatment benefit duration and (right) spectral photoresponse.

Photoresponse for both detector types was unchanged by room-temperature irradiation within the uncertainty, which we estimate from the scatter as about 10%. This uncertainty arises because the detector LCC needed to be removed from the cryostat to send for irradiations. After irradiation, reinstallation in the cryostat, and return of the cryostat to the optical set-up, the optical alignment and thermal coupling were imperfectly reproduced. In contrast, the photoresponse measurements that followed in-situ forward bias injections involved no optical or thermal changes, and consequently had only a few percent uncertainty attributed to temperature drift over several hours. No effect from injection larger than this few percent uncertainty was observed, and any small changes were the same as for untreated control detectors. Thus, the improvements to diffusion length seen in Figure 1 appear to have no effect on photoresponse, which suggests that quantum efficiency is insensitive to L in the G13-141 processed detectors. Whether EB3108 photoresponse depends on diffusion length is unknown since neither diffusion length nor photoresponse changed after room-temperature irradiation and low temperature injection.

Figure 2 (right) presents characteristic photoresponse spectra. The shape of these spectra was unchanged by the room-temperature gamma irradiations. Neither shape nor magnitude of the spectral response were affected by in-situ forward bias injection treatments within experimental uncertainty.

In processed detectors maintained at 77 K during irradiation, absence of room temperature annealing should lead to a more drastic decrease in L. Samples can only be loaded into the EBIC chamber at room temperature, but in-situ photoresponse can be measured without warming up and may finally reveal significant changes to photoresponse. This hypothesis informed the next set of experiments.

Figure 3 presents photoresponse vs cumulative gamma dose at 77 K. For G13-141, there is no change in photoresponse up to more than 700 krad(Si). In contrast, photoresponse for EB3108 decreases by 19%. For each set of detectors, after each of the final few doses, forward-bias injection was applied to one detector, whose photoresponse was then remeasured, while a control detector on the same die was monitored. The treatment comprised 10 mA forward bias for 2 minutes, for an injected charge of order 5 A-s/mm^2. No significant effect and no significant difference between treated and control detectors were observed.

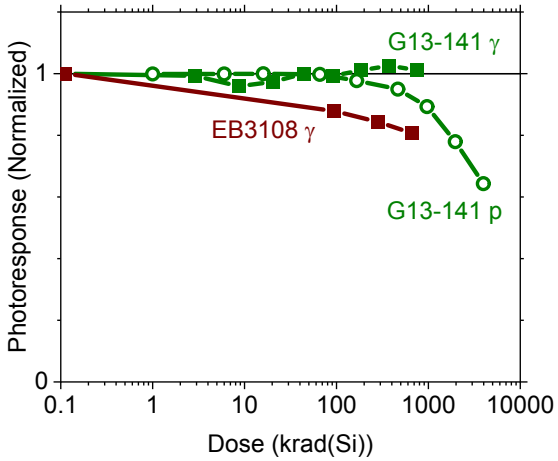

Figure 3. Photoresponse vs ^{60}Co gamma or 30 MeV proton dose.

Next, we repeated the experiments on G13-141 using proton irradiation. Figure 3 presents photoresponse normalized to the pre-irradiated value for one of the 9 detectors studied. Beyond 200 krad(Si), a plot with linear axes shows that the photoresponse degrades linearly with dose. All the detectors on the same die behaved similarly with the maximum degradation being 28-36%. Forward bias injection treatment experiments were performed as before. No change in photoresponse was observed within the few tenths of a percent uncertainty.

SUMMARY

We concluded that G13-141 photoresponse is not limited by minority carrier diffusion, because this photoresponse was insensitive to changes of diffusion length in the range 0.7 to 20 μm. This suggests that the absorption coefficient of the absorber is sufficiently high that the bulk of the carriers are photo-generated within one diffusion length of the contact layer. For the superlattice absorber of G13-141, the absorption coefficient is not independently known. However, since the smallest L value measured by EBIC was 0.7 μm, the absence of any photoresponse effects suggests that the absorption coefficient should be about 1.4 μm^{-1}. Expressions for QE as a function of absorption coefficient and diffusion length [8,9] support this explanation.

The ~1 μm minority carrier diffusion length determined for the absorber region of EB3108 by EBIC is much shorter than values estimated previously for similar devices. A value of 25 um was obtained for low-doped InAsSb from analysis of photoresponse dependence on mesa size for backside-illuminated detectors, where diffusion is lateral from the unpatterned InSbAs absorber-layer regions surrounding the mesa [10]. An assumption in the calculations of [10] is that all carriers excited by radiation absorbed in the absorber layer under the biased mesa contribute to photoresponse, and that the majority of such carriers contribute even at zero bias because of the large diffusion length. In contrast, our EBIC measurements on unbiased EB3108 indicate that the collected fraction of carriers excited by the electron beam falls rapidly with distance into the absorber layer. Our L value from EBIC was unaffected by either room temperature irradiation or injection treatment. Whether it was affected by low-temperature irradiation or treatment remains unknown because EBIC could not be performed in-situ during low-temperature irradiations. The decrease in EB3108 photoresponse caused by gamma irradiation at 77 K may have been due to degraded minority carrier diffusion, however minority carrier injection provided no recovery to photoresponse.

In conclusion, our experiments thus far indicate that forward bias minority carrier injection can provide long-lasting mitigation for minority carrier diffusion degraded by radiation damage in certain heterojunction barrier infrared detector structures. However, this effect lacks a corresponding improvement in photoresponse, in contrast to the situation observed for wide-gap UV photodiodes.

Acknowledgments and disclosure

Truventic and UCF authors acknowledge support from Missile Defense Agency SBIR Contract HQ014718C7310 (Program Manager Eric Luft). CJF and REP have a financial interest in Truventic, and these authors may profit from the results of this research. Sandia National Laboratories is a multimission laboratory managed and operated by National Technology & Engineering Solutions of Sandia, LLC, a wholly owned subsidiary of Honeywell International Inc., for the U.S. Department of Energy's National Nuclear Security Administration under

contract DE-NA0003525. This paper describes objective technical results and analysis. Any subjective views or opinions that might be expressed in the paper do not necessarily represent the views of the U.S. Department of Energy or the United States Government.

References

1. Missile Defense Agency SBIR solicitation topic #16-011, "Radiation Hardened Interceptor Seeker Sensor Technologies" (2016).
2. B. R. Bhat, N. Upadhyaya, and R. Kulkarni, "Total Radiation Dose at Geostationary Orbit," IEEE Trans. Nuclear Science 52, 530 (2005).
3. O. Lopatiuk-Tirpak, L. Chernyak, L.J. Mandalapu, Z. Yang, J.L. Liu, K. Gartsman, Y. Feldman, Z. Dashevsky, "Influence of electron injection on the photoresponse of ZnO homojunction diodes", Appl. Phys. Lett., 89, 142114 (2006).
4. L. Chernyak, W. Burdett, "Electron injection-induced effects in GaN: Physics and Applications", MRS Spring Meeting Proceedings, 764, C5.4 (2003).
5. C. Fredricksen, R. E. Peale, L. Chernyak, J. Lee, "Radiation-defect mitigation in InAs/GaSb strained-layer superlattice infrared detectors," SBIR Phase I final report, Missile Defense Agency, Contract # HQ0147-17-C-7256, June 9, 2017.
6. C. Fredricksen, R. E. Peale, L. Chernyak, J. Lee, "Radiation-defect mitigation in InAs/GaSb strained-layer superlattice infrared detectors" SBIR Phase I Option final report, Missile Defense Agency, Contract # HQ0147-17-C-7256, March 21, 2018.
7. J. F. Klem, J. K. Kim, M. J. Cich, S. D. Hawkins, T. R. Fortune, J. L. Rienstra, "Comparison of nBn and nBp mid-wave barrier infrared photodetectors," Proc. SPIE 7608, 76081P (2010).
8. E. Giard, I. Ribet-Mohamed, J. Jaeck, T. Viale, R. Haidar, R. Taalat, M. Delmas, J.-B. Rodriguez, E. Steveler, N. Bardou, F. Boulard, and P. Christol, "Quantum efficiency investigations of type-II InAs/GaSb midwave infrared superlattice photodetectors," J. Appl. Phys. 116, 043101 (2014).
9. B.-M. Nguyen, D. Hoffman, Y. Wei, P-Y. Delaunay, A. Hood, and M. Razeghi, "Very high quantum efficiency in type-II InAs/GaSb superlattice photodiode with cutoff of 12 μm," Appl. Phys. Lett. 90, 231108 (2007).
10. P. Klipstein, O. Klin, S. Grossman, N. Snapi, B. Yaakobovitz, M. Brumer, I. Lukomsky, D. Aronov, M. Yassen, B. Yofis, A. Glozman, T. Fishman, E. Berkowicz, O. Magen, I. Shtrichman, and E. Weiss, ""XBn" Barrier Detectors for High Operating Temperatures," Proc. SPIE 7608, 76081V (2010).